Monte Carlo Simulations of a Single Polyelectrolyte in Solution: Activity Coefficients of the Simple Ions and Application to Viscosity Measurements

Magnus Ullner,† Georges Staikos, and Doros N. Theodorou*

Department of Chemical Engineering, University of Patras and Institute of Chemical Engineering and High-Temperature Chemical Processes, GR-26500 Patras, Greece

Received March 20, 1998; Revised Manuscript Received August 12, 1998

ABSTRACT: Monte Carlo simulations of linear polyelectrolytes together with explicit ions have been performed in a spherical cell model to study conformational changes and activity coefficients in relation to the isoionic dilution method used in viscosity measurements. The results show that it is possible to define an effective ionic strength that will keep the average chain conformation constant on isoionic dilution and that this ionic strength can be predicted from the activity of the counterions, as has been suggested experimentally. Activity coefficients have been calculated from the simulations and compared with theoretical estimates based on various applications of the Debye−Hückel approximation, including Manning theory and an expression for a rigid rod with discrete charges. Manning theory generally gives poor agreement with the simulations, while the rigid-rod expression, which includes an ion−ion term, is able to predict the mean activity coefficient at not too high charge densities. Assuming that the co-ions are completely inert, the rigid-rod expression also leads to a reasonable approximation for the counterion activity. The simulation results have been used as input for two theoretical expressions for the reduced viscosity. The first, which is only based on the average chain conformation, does not reproduce the qualitative features of experimental curves. Our chains, with only 80 monomers, do not display large conformational changes upon dilution with salt solutions of varying ionic strength. In contrast, the second viscosity expression, which takes intermolecular electrostatic interactions into account, gives a correct qualitative behavior.

Introduction

When a neutral polymer is diluted, the reduced viscosity, η_r, can in general be described with the linear Huggins equation,[1]

$$\eta_r \equiv \frac{\eta - \eta_0}{\eta_0 c_p} = [\eta] + k_H[\eta]^2 c_p \qquad (1)$$

where η is the viscosity of the solution and η_0 that of the solvent. The intrinsic viscosity, $[\eta]$, and the Huggins coefficient, k_H, can thus be obtained from a plot of the reduced viscosity, η_r, against the polymer concentration, c_p.

For polyelectrolytes, the situation is usually not that simple. At low ionic strengths of the diluent, the reduced viscosity increases on dilution, and a maximum can be observed before the reduced viscosity heads for its value at infinite dilution, $[\eta]$.[2,3] This increase in η_r is known as the polyelectrolyte effect.

If solutions of increasingly higher ionic strengths are used for the dilution, the peak is reduced. Eventually the maximum disappears completely, and if the ionic strength of the initial polyelectrolyte solution is lower than that of the diluent, there may even be a sharp decrease in the reduced viscosity at the onset of dilution.[3,4] Pals and Hermans showed that it was possible to choose an ionic strength for the diluting solution such that straight lines analogous to eq 1 were obtained[5,6] but with an apparent Huggins coefficient that could be much larger than for neutral polymers. A linear behavior is of course desirable in the extrapolation to $c_p = 0$ to obtain $[\eta]$.

The intrinsic viscosity depends on the size and shape of the molecule. For example, for a neutral, nondraining polymer, the expected behavior is $[\eta] \propto R_G^3$, which looks like the result for a sphere with a radius proportional to the radius of gyration, R_G.[7,8] With neutral polymers in mind, it is not surprising that the polyelectrolyte effect has traditionally been explained as a rapid increase in chain dimensions. The effect of added salt is then to screen the intramolecular interactions and make the chain expand less strongly. The rationale for the Pals and Hermans dilution was thus to keep the average conformation of the chain constant by keeping the ionic strength constant. Their isoionic strength dilution is now known as isoionic dilution, for short.

Sometimes the polyelectrolyte effect has been presented as an equilibrium between "free" counterions and counterions "bound" to the macroion.[3,7] When the dilution is performed with a low ionic strength solution, the counterions are diluted away from the polyelectrolyte, which increases the "net charge" and subsequently the dimensions of the macroion. The isoionic dilution would then retain the balance between "free" and "bound" ions. Although this explanation is somewhat oversimplified, it focuses the attention on the counterions and suggests that the ionic strength for the dilution would be directly obtainable from an estimate of the counterion activity, as opposed to the original trial and error procedure.[3,5,6] The use of Manning theory for such a direct prediction has been experimentally successful for poly(styrene sulfonate)[9] and poly(acrylic acid).[4,10]

* To whom correspondence should be addressed.
† Present address: School of Chemistry, University College ADFA, University of New South Wales, Canberra ACT 2600, Australia.

10.1021/ma9804388 CCC: $15.00
Published on Web 10/13/1998

We will combine the conformational interpretation of the polyelectrolyte effect with the idea that the counterions are of special importance and ask the question: Is it possible to use the counterion activity to define an effective ionic strength that will keep the average chain conformation constant during an isoionic dilution?

As we will see, the answer is yes, but it should be pointed out that it does not prove that the intramolecular interactions are the main cause of the polyelectrolyte effect. The intermolecular interactions may also stay constant, and there are strong indications that these are largely responsible for the effect.[2,11−17] For example, latices,[14,15] telechelic ionomers with a charge at just one end,[16] and spherical poly(styrene sulfonate) particles[17] all have a more or less fixed size but can still display a behavior similar to that of flexible polyelectrolytes, which points toward an explanation in terms of intermolecular interactions.

There are several length scales in the system: the Debye screening length, κ^{-1}, which measures the range of the electrostatic interactions, the radius of gyration, R_G, and the average distance between the polyelectrolytes, D, assuming that polyelectrolyte molecules are roughly arranged on a cubic lattice. For the conformational interpretation of the polyelectrolyte effect, an important quantity is the ratio between the first two length scales. If $\kappa R_G < 1$, the whole chain is interacting with itself, but if this ratio is larger than 1, the electrostatic interactions extend only over parts of the chain. In the latter case, when the ionic strength is lowered, κ^{-1} increases, the chain sections that interact with themselves get bigger, the total electrostatic repulsion grows, and the chain expands. This is what the conformational interpretation envisions when a polyelectrolyte is diluted with a salt solution of low ionic strength. The expansion leads to an increase in $[\eta]$.

For the intermolecular electrostatic interactions, the ratio κD indicates if it is sufficient to treat them as pairwise ($\kappa D > 1$) or if multimolecule interactions have to be considered as well. κD is about 3−5 at the highest polyelectrolyte concentration in most of our model systems. In the pairwise regime, κR_G is once again relevant to determine how much the intermolecular interactions influence the viscosity. Even though the polyelectrolytes may be far apart on average, κR_G is important, because the reduced viscosity depends on the whole range of possible interactions. If $\kappa R_G \ll 1$ and a macroion is approaching another, what it sees is basically a sphere with a radius on the order of κ^{-1}. A larger radius means a larger reduced viscosity. If the chain size is insignificant compared to κ^{-1}, intermolecular electrostatic interactions should therefore dominate the viscous behavior. The difference in the hydrodynamic radius seen by the solvent and the effective radius seen by other macroions goes into the Huggins coefficient.[18]

Our simulations do not measure the viscosity, but there are theories that predict the reduced viscosity from quantities that are obtained in the simulations, for example, the radius of gyration and the effective ionic strength. We will use two such expressions, one based on the average size of the chain, the other based on intermolecular electrostatic interactions, to see if these hypothetical viscosities are able to reproduce the experimentally observed behavior. Note that we are not simulating macroion−macroion interactions. These are only taken care of implicitly via the second theory.

With the experimental success of Manning theory as a predictor of activity coefficients for the isoionic dilution,[4,9,10] it is of interest to explore its ability to reproduce the simulation results. The Manning expressions were originally derived for an infinite line charge,[19] but a better test for the Debye−Hückel approximation, on which Manning theory relies, would be a model closer to the one used in the simulations. We will therefore make a comparison with the Debye−Hückel result for a finite chain with discrete charges, which also includes an ion−ion term.

In the two following sections we will describe the simulation model and the details of the simulations. The discussion of the results starts by addressing the question about the connection between isoionic dilution, counterion activity, and chain conformation. This is followed by an investigation of activity coefficients as predicted by the Debye−Hückel approximation and by Manning theory and their comparison with simulation results. Finally, we employ viscosity theory to test if a conformational interpretation of the polyelectrolyte effect or one based on intermolecular interactions gives the most realistic behavior when a hypothetical reduced viscosity is calculated from our simulation data.

Simulation Model

The simulations are based on a cell model.[20−23] A polyelectrolyte solution of finite concentration is thought of as being divided into cells corresponding to the average volume per chain, $V = 1/(N_A c_p')$, where N_A is Avogadro's number and c_p' is the molar concentration of the polyelectrolyte. Our system consists of a linear polyelectrolyte with $N = 80$ monomers together with simple ions, contained in a spherical cell centered on monomer $N/2$. The polyelectrolyte concentration will be expressed in terms of the monomer concentration $c_p = N c_p'$. The polyelectrolyte is modeled as a freely jointed chain with rigid bonds of length b. Each monomer is a hard sphere and has a fractional charge corresponding to an average degree of neutralization α. Simulations of titrating polyelectrolytes have shown that a fractional charge on every monomer is a good approximation for partly dissociated chains.[24,25]

Within the cell we use the primitive model, i.e., the ions are treated explicitly as hard spheres, while the solvent (water) is treated as a dielectric continuum with dielectric constant ϵ_r. The total interaction energy is

$$E = E^{el} + E^{hs} = \sum_{i<j} \frac{z_i z_j e^2}{4\pi\epsilon_r\epsilon_0 r_{ij}} + \sum_{i<j} u^{hs}(r_{ij}) \qquad (2)$$

where the sums extend over all pairs of monomers and ions. z_i is the valency of site i. Assuming a polyacid, the monomers have $z_p = -\alpha$. The simple ions are all monovalent, i.e., $|z_i| = 1$. e is the elementary charge, ϵ_0 the permittivity of vacuum, r_{ij} the distance between sites i and j, and

$$u^{hs}(r) = \begin{cases} \infty & r < \sigma \\ 0 & r \le \sigma \end{cases} \qquad (3)$$

is the hard-sphere pair interaction potential. All monomers and ions have a distance of closest approach σ of 4 Å. The simulations are performed at a temperature $T = 298$ K and with $\epsilon_r = 78.3$, which gives a Bjerrum length $l_B = e^2/(4\pi\epsilon_r\epsilon_0 k_B T)$ of about 7.16 Å. k_B is Boltzmann's constant.

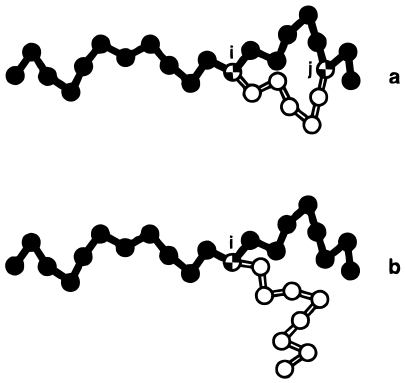

Figure 1. Schematic representation of (a) the crankshaft rotation and (b) the pivot move. In the crankshaft move, the chain between two randomly picked monomers, *i* and *j*, is rotated around the axis joining the two monomers. The empty spheres represent the positions of the rotated monomers in the new trial conformation. In the pivot move, the whole chain from a chosen monomer, *i*, to the nearest end is rotated around monomer *i*.

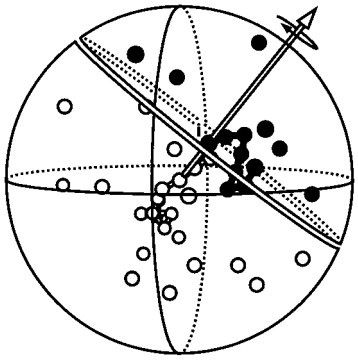

Figure 2. Schematic representation of the cap rotation. A spherical cap is defined by a plane through a randomly chosen monomer, *i*, and a vector from the center of the cell (monomer $N/2$) passing through monomer *i*. As a trial move, all the simple ions within this cap will be rotated together with monomers *i* to N, if $i \geq N/2$, or monomers 1 to *i*, if $i < N/2$, around the axis formed by the vector. (If $i = N/2$, a random vector is chosen.) The atoms to be rotated are represented by filled spheres.

The cell wall has a distance of closest approach of 0, i.e., an ion may have its "center of mass" at the position of the wall. This applies also to the monomers, but in none of the reported cases are the chain conformations biased by contacts with the cell boundary. There are no interactions with anything outside the cell. Correlations between the cells that implicitly make up the total (macroscopic) solution are thus neglected, although they are to some extent included in a correction for the finite size of the cell in the calculation of the chemical potentials. Simulations comparing a cell model and an isotropic solution of spherical micelles have shown that the cell model is a good approximation at low polyelectrolyte concentrations.[26]

Monte Carlo Simulations

Algorithms. The Monte Carlo (MC) simulations are performed with the traditional Metropolis algorithm.[27] Originally, the chain conformations were only sampled using a pivot algorithm for the chain itself.[28,29] In this scheme, a monomer is picked to act as origin for a rigid-body rotation of the part of the chain that extends from the selected monomer to the nearest end (see Figure 1b). (Since monomer $N/2$ is fixed at the center of the cell, a change of conformation is always attempted on one or the other side of the middle of the chain, never across the central bead.) A rotation axis is also chosen at random. Although this has proven to be a very good algorithm for a system with just the single chain,[30] it was found that the presence of simple ions does not just bring down the acceptance ratio and force an increase in the length of the simulation but may even trap the chain in a subset of conformations that will persist for a large part of the simulation. Increasing the length of the run can in this case be a waste of time. This occurs mainly when the charge density of the polyelectrolyte is very high, and the resulting high, local concentration of counterions will prevent any substantial rotation in the central part of the chain. Christos and Carnie have also reported problems, to the extent that results had to be discarded, when they simulated fully ionized polyelectrolytes with explicit salt, but they used the slithering snake algorithm (reptation).[31]

Gordon and Valleau have devised a modified pivot algorithm where part of the ion atmosphere is rotated together with the chain.[32] The gain in trial configurations is partly counteracted by the extra time needed to select ions within a certain radius of the chain. Gordon and Valleau reported a 60% increase in the CPU time required to generate the Markov chain itself while gaining a factor of 2−5 in an improved convergence rate for the conformational properties. To get out of our bottlenecks, we have introduced a move that is similar in spirit, but simpler. Our move, which we call a "cap rotation", is perhaps more related to a crankshaft move (see Figure 1a) than to a proper pivot, because it is more deterministic and less perturbing to the system. The rotation axis is given by the vector from the center of the cell to a randomly selected monomer, *i*. This vector, together with the monomer, defines a plane (perpendicular to the axis). All simple ions above this plane (in the direction of the vector) are rotated together with the part of the chain extending from the selected monomer to the nearest end. This is illustrated in Figure 2, where the filled atoms are those that will be rotated. The move may be thought of as rotating a spherical cap of the cell, although it is possible that a rotated part of the chain is outside the spherical cap and a stationary part may be inside it. In these cases, it is still possible that the chain overlaps with itself or simple ions after the rotation. This is most likely in the case of a trial move around the central monomer, where a random rotation vector is used. A normal crankshaft move (explained in Figure 1a) has also been added. No simple ion is rotated in a crankshaft move.

To summarize, we have used three moves that change the conformation of the polyelectrolyte: the chain-only pivot around a random rotation vector, the cap rotation, and the crankshaft. Any attempted rotation is randomly picked within a full circle. The choice of move is also random, with the cap rotation being selected on average one-fourth of the time. The other two ways of changing conformation are biased, so that a crankshaft is attempted more often in the middle section of the chain, where the pivot is more likely to fail.

The new procedure has not been optimized for efficiency, i.e., precision/simulation time, but the computational cost is very similar for the three different moves, and the efficiency seems to be comparable to that of the original pivot in the case of low ion density. The results are also the same. Furthermore, we have tested

that different starting conformations do not bias the results. The advantage is that the new scheme avoids the bottlenecks at high ion densities. The inclusion of the cap rotation makes high-density simulations with different seeds for the random-number generator converge to the same results.

A simulation cycle consists of trying to move one-fourth of the simple ions individually and attempting one chain-perturbing move. A full simulation contains up to 5×10^5 cycles per bond, or 4×10^6 cycles in total for the 80-mer. CPU times on an IBM RS/6000 43P workstation range from a few hours to weeks, depending on the combination of cell radius and salt concentration. Estimated standard deviations of around 1% or better for the conformational properties are needed to get dilution curves where the conformational trends are not overshadowed by fluctuations of the averages.

Chemical Potential. Chemical potentials for the simple ions are calculated using Widom's method[33] with a correction for nonelectroneutral insertions into a finite volume.[34] A test particle, which does not perturb the system, is randomly inserted, and its interactions with all the real solute particles are calculated to give the excess chemical potential, μ_l^{ex}. These interactions, U_l, depend on which species, l, the test particle represents and the (dimensionless) excess chemical potential is obtained as

$$\beta\mu_l^{\mathrm{ex}} = -\ln\langle\exp[-\beta U_l^{\mathrm{hs}}]\rangle + \int_0^1 \mathrm{d}\lambda \frac{\langle\beta U_l^{\mathrm{el}} \exp[-\beta(U_l^{\mathrm{hs}} + \lambda U_l^{\mathrm{el}})]\rangle}{\langle\exp[-\beta(U_l^{\mathrm{hs}} + \lambda U_l^{\mathrm{el}})]\rangle} \quad (4)$$

where $\beta \equiv (k_B T)^{-1}$ and the angular brackets denote ensemble averages over all equilibrium configurations of the real particles, accumulated in the course of a MC run. The last term represents a charging process that contains the correction.[34] During this process, electroneutrality is maintained by rescaling every charge z_j with the factor $1 - \lambda z_l/(z_j N_z)$, where N_z is the total number of charged particles in the cell. The rescaling is a necessary modification of U_l^{el}, because our finite system is not able to accommodate an inserted full charge the same way as an infinite system would. The rescaling may thus be viewed as a reaction from the surroundings that are not explicitly simulated. In practice we calculate the integral in eq 4 from 11 points using the extended Simpson's rule.[35]

The total chemical potential is

$$\beta\mu_l = \beta\mu_l^{\dagger} + \ln a_l = \beta\mu_l^{\dagger} + \ln c_l + \ln \gamma_l \quad (5)$$

where $\mu_l^{\dagger}$ is the standard chemical potential (chemical potential of species l in an ideal solution of unit molar concentration of l) and a_l is the activity, which in an ideal solution equals the molar concentration c_l. By an ideal solution, we here mean a solution where there are no solute−solute interactions, and as the "real" solution becomes more dilute, it will approach ideality, i.e., $\gamma_l \to 1$ when $c_l \to 0$ simultaneously for all solute species. The activity coefficient γ_l represents the excess part

$$\ln \gamma_l = \beta\mu_l^{\mathrm{ex}} \quad (6)$$

Results and Discussion

The following discussion will be limited to the case where the free ions are monovalent and the counterions from the salt are the same as those from the polyelectrolyte itself; this is the case studied with our model system. Not only does this simplify the equations, but the Debye−Hückel theory would be doomed from the start if multivalent ions were present, because it neglects ion−ion correlations that are important for divalent ions.[36] With counterions and co-ions denoted by the subscripts 1 and 2, respectively, the total counterion concentration can be expressed as $c_1 = \alpha c_p + c_s$, where c_s ($=c_2$) is the concentration of the added salt.

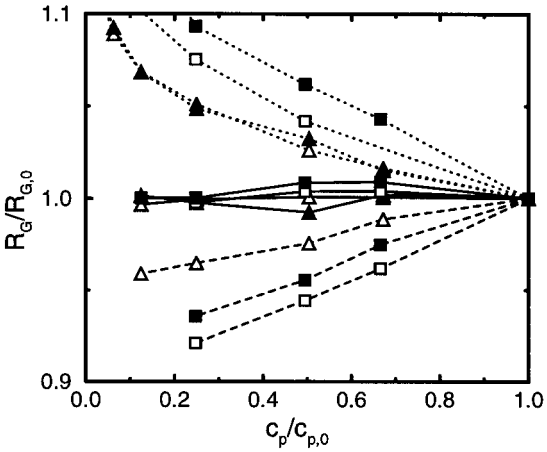

Figure 3. Conformational change on dilution. $R_{G,0}$ and $c_{p,0}$ are the radius of gyration and the polyelectrolyte concentration at the start of the dilution. Data are shown for bond lengths $b = 3$ Å (triangles) and $b = 6$ Å (squares) and degrees of dissociation $\alpha = 0.5$ (open symbols) and $\alpha = 1$ (filled symbols). Dotted lines represent dilution with zero ionic strength and dashed lines with an ionic strength of 5 mM, while solid lines show isoionic dilution (eq 8) with 2.1 and 2.5 mM for $b = 3$ Å with $\alpha = 0.5$ and $\alpha = 1$, respectively, and 1.4 and 2.0 mM for $b = 6$ Å.

Isoionic Dilution. To have an isoionic dilution, we first need to define an effective ionic strength, I_{eff}. The basic assumptions are that the co-ions are more or less inert and that the counterions should not notice any difference between a pure salt solution with a concentration $c_{\mathrm{eff}} = I_{\mathrm{eff}}$ and the polyelectrolyte solution where the counterion concentration is c_1. The difference in chemical potential $\beta\Delta\mu_1$ between the two solutions should thus be 0, and with the further approximation that c_{eff} is low enough to treat the pure salt solution as ideal, we have

$$\beta\Delta\mu_1 = \ln(\gamma_1 c_1/c_{\mathrm{eff}}) = 0 \quad (7)$$

which gives

$$I_{\mathrm{eff}} = c_{\mathrm{eff}} = \gamma_1 c_1 \quad (8)$$

This has been the starting point when Manning theory has been employed to predict the appropriate salt concentration for the isoionic dilution.[4,9,10] Since we can determine the activity coefficient directly from the simulations, we do not need further approximations to test eq 8, and we will save a comparison with Manning theory until later.

Let us start with the assumption that a constant chemical potential for the counterions will keep the average chain conformation constant. Figure 3 shows how the radius of gyration, R_G, changes when the polyelectrolyte is diluted by adding volumes of a 1:1 salt solution of a given ionic strength, i.e., when the cell radius is increased and ion pairs are added as if the

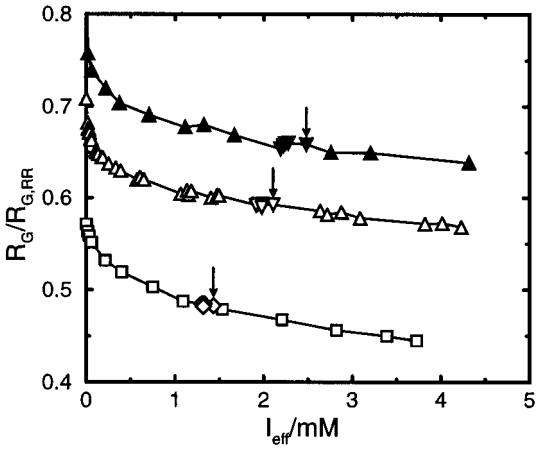

Figure 4. Radius of gyration plotted against the effective ionic strength, $I_{eff} = \gamma_1 c_1$, for various combinations of c_p and c_s. The radius of gyration is scaled by the value it would have if the chain were fully extended, i.e., a rigid rod, $R_{G,RR}^2 = (N^2 - 1) \cdot b/12$. The polyelectrolyte concentration, c_p, ranges from 3×10^{-8} to 9.8 mM, and the concentration of the added salt, c_s, is between 0 and 4.4 mM. Data are shown for $b = 3$ Å (triangles) and $b = 6$ Å (squares and diamonds) with $\alpha = 0.5$ (open symbols) and $\alpha = 1$ (filled symbols). Triangles pointing down and diamonds represent isoionic dilution with the starting point marked by an arrow.

extra volume had contained salt of a specific concentration. The radius of gyration is defined as

$$R_G^2 \equiv \frac{1}{N}\sum_{i=1}^{N}\langle(\mathbf{r}_i - \mathbf{r}_{cm})^2\rangle = \frac{1}{N^2}\sum_{i=1}^{N-1}\sum_{j=i+1}^{N}\langle r^2_{ij}\rangle, \qquad (9)$$

where $\mathbf{r}_{cm}$ is the center of mass coordinate and r_{ij} is the distance between monomers i and j. As the figure shows, when we use the concentration obtained from eq 8 at the salt-free starting point (a simulation of just the polyelectrolyte and its neutralizing counterions), R_G stays roughly constant. Another salt concentration for the diluent leads to an expansion or contraction of the chain, depending on whether it is lower or higher, respectively, than I_{eff}.

Figure 4 confirms that R_G is a continuous function of $I_{eff} = \gamma_1 c_1$. I_{eff} itself varies as a function of the concentrations of polyelectrolyte and added salt, but despite large changes in these concentrations and in the ratio between them, all the points (I_{eff}, R_G) fall onto a single curve (within the precision of the simulations) for a given polyelectrolyte, specified by b and α. I_{eff} should also stay constant during the isoionic dilution, and so it does once salt has been added, but it is slightly higher at the initial, salt-free point (marked by an arrow), which was the value used for the whole isoionic dilution. Our definition of the effective ionic strength is therefore not optimal, but that has little effect on the radius of gyration or, for that matter, on $I_{eff} = \gamma_1 c_1$ after the first addition of salt.

It was assumed initially that the co-ions should be more or less inert, and this is also what the simulations show. The activity coefficient of the co-ions is not affected much by the presence of the polyelectrolyte. In all the points shown in Figure 4, γ_2 stays within the range 0.90−1.15, while γ_1 varies between 0.25 and 1.0. This corroborates that it is mainly the counterions that interact with the polyelectrolyte and modify its effective intramolecular interactions, which is the reason for the strong connection between the counterion activity and the polyelectrolyte conformations.

Our model with $b = 3$ Å roughly corresponds to poly(acrylic acid), where the projected length of a monomer along the backbone is 2.52 Å. For $\alpha = 0.5$ we obtained $I_{eff} = 2.1$ mM, which is exactly the same value as was reported from experimental measurements on a sample of poly(acrylic acid) with the same initial, "salt-free" concentration and the same degree of dissociation, although the degree of polymerization of the real chain was about 7 times larger than here (experimental curve shown in Figure 12).[4]

Activity Coefficients. Based on Debye−Hückel theory, Manning has given the following expressions for the activity coefficient of the counterion.[19]

$$\ln \gamma_1 = -\frac{1}{2}\xi\frac{\alpha c_p}{\alpha c_p + 2c_s} \text{ for } \xi < 1 \qquad (10)$$

$$\gamma_1' = \frac{\xi^{-1}\alpha c_p + c_s}{\alpha c_p + c_s}\exp\left[-\frac{\xi^{-1}\alpha c_p}{2(\xi^{-1}\alpha c_p + 2c_s)}\right] \text{ for } \xi > 1 \qquad (11)$$

In the case of no added salt, this reduces to

$$\ln \gamma_1 = -\frac{1}{2}\xi \text{ for } \xi < 1 \qquad (12)$$

$$\gamma_1' = \xi^{-1}e^{-1/2} \text{ for } \xi > 1 \qquad (13)$$

The prime indicates a result of Manning rescaling. According to Manning theory,[19,37] when the parameter $\xi = \alpha l_B/b$ exceeds 1, there will always be a certain amount of counterions in the vicinity of the polyelectrolyte to neutralize a fraction $1 - \xi^{-1}$ of its charge, i.e., to give an effective charge density $\xi' = 1$, which is the same as setting the degree of ionization to $\alpha' = b/l_B$. The point is to extend the range of a Debye−Hückel-like description to higher charge densities, where the Debye−Hückel approximation is expected to fail. A detailed description of the procedure for obtaining rescaled activity coefficients according to Manning is given in appendix A.

Comparison between Manning theory and simulation can be found in Tables 1 and 2 as well as in Figures 5 and 6. Note that the Debye−Hückel approximation leads to the same value for the activity coefficients for the counterions and the co-ions, i.e., $\gamma_1 = \gamma_2$ (an important point, which we will return to), and the mean activity coefficient $\gamma_\pm = \sqrt{\gamma_1\gamma_2}$ is therefore also given by eqs 10 and 12. (With Manning rescaling γ_1 and $\gamma_\pm$ are different, cf. Appendix A.) Note also that, since the excess chemical potential is measured with a test particle in the simulations, there do not need to be any co-ions present to measure γ_2.

Perhaps most striking is the disagreement between Manning theory and simulation in the salt-free case (see, for example, Figure 5a), where eqs 12 and 13 claim that the activity coefficient is independent of polyelectrolyte concentration. This is obviously not the case, although the circles in Figure 7 show that the activity coefficient is almost constant at the highest polyelectrolyte concentrations. The larger changes come when the polymer begins to be highly diluted. The higher the charge density, the smaller the variation in activity coefficient at high c_p.

Table 1. Counterion and Mean Ion Activity Coefficients in Cell Model Simulations (MC) of a Polyelectrolyte with 3 Å Bonds, Compared to the Predictions of Manning Theory (Eq 10), a Rigid-Rod Model with Discrete Charges and Finite Length (Eq 14), and the Rigid Rod with the Manning and Zimm Correction for the Difference in Single-Ion Activities (Eq 16)[a]

					MC		eq 10			eq 14			eq 16	
b (Å)	α	ξ	c_p (mM)	c_s (mM)	γ_1	$\gamma_\pm$	γ	γ'_1	$\gamma'_\pm$	γ	γ'_1	$\gamma'_\pm$	γ_1	γ'_1
3	0.2	0.48	9.78	0.00	0.71	0.87	0.79			0.83			0.69	
				0.98	0.74	0.89	0.89			0.87			0.80	
				10.00	0.82	0.88	0.98			0.87			0.86	
				100.00	0.77	0.79	1.00			0.69			0.69	
			2.44	0.00	0.79	0.92	0.79			0.89			0.71	
				0.98	0.84	0.93	0.95			0.93			0.90	
	0.5	1.19	9.78	0.00	0.43	0.70	0.55	0.51	0.56	0.60	0.55	0.60	0.22	0.26
				0.98	0.49	0.73	0.65	0.62	0.66	0.67	0.62	0.67	0.34	0.39
				10.00	0.68	0.82	0.89	0.87	0.89	0.79	0.77	0.79	0.69	0.71
				100.00	0.76	0.78	0.99	0.98	0.99	0.68	0.67	0.68	0.67	0.67
			2.44	0.00	0.50	0.75	0.55	0.51	0.56	0.70	0.62	0.68	0.20	0.25
				0.98	0.64	0.82	0.80	0.77	0.80	0.81	0.77	0.81	0.53	0.59
				2.50	0.73	0.86	0.89	0.87	0.89	0.86	0.83	0.85	0.71	0.74
			0.62	0.00	0.58	0.80	0.55	0.51	0.56	0.79	0.70	0.76	0.19	0.25
			0.04	0.00	0.82	0.93	0.55	0.51	0.56	0.93	0.79	0.87	0.17	0.24
			3×10^{-8}	0.00	1.00	1.00	0.55	0.51	0.56	1.00	0.84	0.91	0.15	0.22
	1.0	2.39	9.78	0.00	0.25	0.54	0.30	0.25	0.39	0.35	0.28	0.43	0.01	0.13
				0.98	0.30	0.58	0.37	0.34	0.49	0.40	0.34	0.50	0.02	0.21
				2.45	0.35	0.62	0.45	0.43	0.58	0.46	0.41	0.56	0.06	0.31
			2.44	0.00	0.29	0.57	0.30	0.25	0.39	0.44	0.31	0.48	0.00	0.13
				0.98	0.43	0.68	0.52	0.49	0.64	0.58	0.50	0.65	0.06	0.38
				2.50	0.56	0.76	0.68	0.65	0.78	0.68	0.63	0.74	0.20	0.56
			0.62	0.00	0.36	0.63	0.30	0.25	0.39	0.57	0.35	0.54	0.00	0.12
			0.04	0.00	0.50	0.73	0.30	0.25	0.39	0.83	0.40	0.61	0.00	0.12
			3×10^{-8}	0.00	1.00	1.00	0.30	0.25	0.39	1.00	0.42	0.65	0.00	0.11

[a] γ is the result of the equation indicated. It has been interpreted as γ_1, but it is better viewed as $\gamma_\pm$ (see text). γ'_1 is the activity coefficient for the counterions if Manning rescaling is used (to be applied at $\xi > 1$) and $\gamma'_\pm$ is the corresponding mean activity coefficient.

Table 2. Activity Coefficients as in Table 1, But Based on a Polyelectrolyte with a Bond Length of 6 Å

					MC		eq 10			eq 14			eq 16	
b (Å)	α	ξ	c_p (mM)	c_s (mM)	γ_1	$\gamma_\pm$	γ	γ'_1	$\gamma'_\pm$	γ	γ'_1	$\gamma'_\pm$	γ_1	γ'_1
6	0.2	0.24	4.93	0.00	0.78	0.92	0.89			0.89			0.85	
				0.99	0.81	0.92	0.96			0.92			0.91	
				9.98	0.86	0.89	0.99			0.88			0.89	
			2.44	0.00	0.82	0.94	0.89			0.91			0.86	
				0.98	0.85	0.94	0.98			0.94			0.93	
	0.5	0.60	4.93	0.00	0.58	0.81	0.74			0.75			0.56	
				0.99	0.64	0.83	0.85			0.82			0.71	
				9.98	0.78	0.86	0.97			0.86			0.84	
			2.44	0.00	0.61	0.83	0.74			0.78			0.57	
				0.98	0.70	0.82	0.89			0.87			0.78	
				2.50	0.76	0.88	0.94			0.89			0.85	
			0.62	0.00	0.69	0.88	0.74			0.83			0.58	
			0.04	0.00	0.87	0.96	0.74			0.94			0.62	
			3×10^{-8}	0.00	1.00	1.00	0.74			1.00			0.62	
	1.0	1.19	4.93	0.00	0.40	0.66	0.55	0.51	0.56	0.56	0.52	0.56	0.20	0.25
				0.99	0.46	0.75	0.65	0.62	0.66	0.64	0.60	0.65	0.32	0.38
				2.46	0.52	0.74	0.74	0.71	0.75	0.70	0.67	0.71	0.45	0.50
			2.44	0.00	0.41	0.69	0.55	0.51	0.56	0.59	0.54	0.59	0.19	0.24
				0.98	0.51	0.75	0.72	0.68	0.73	0.71	0.67	0.72	0.40	0.46
				2.50	0.61	0.80	0.82	0.80	0.83	0.78	0.75	0.79	0.57	0.62
			0.62	0.00	0.47	0.73	0.55	0.51	0.56	0.66	0.60	0.65	0.17	0.23
			0.04	0.00	0.64	0.83	0.55	0.51	0.56	0.84	0.73	0.80	0.16	0.23
			3×10^{-8}	0.00	1.00	1.00	0.55	0.51	0.56	1.00	0.84	0.92	0.15	0.22

The prediction of a constant activity coefficient in the absence of added salt is partly retained when only small amounts of salt are added, and the correlation between theory and simulation looks very scattered. The uppermost triangles in Figures 5b and 6b represent dilution with a 0.01 mM salt solution, and the set just below corresponds to a 0.1 mM diluent. Simulations with the very low concentration 0.01 mM were only performed for chains with $b = 3$ Å and $\alpha = 0.5$, which is why the triangles stand out. This particular chain and the one with $b = 6$ Å and $\alpha = 1$ both have $\xi = 1.2$, which explains the close proximity of triangles and circles at the higher concentrations of added salt.

Comparison with solutions to the Poisson−Boltzmann equation has indicated that, although there is nothing wrong with the concept of charge rescaling, the particular form of the Manning rescaling is of limited utility.[38,39] This is also the conclusion here. In the case of γ_1, the Manning rescaling (open symbols in Figure 5) decreases the predicted value, which means that there is an improvement when γ_1 is overestimated, but the error increases when the predicted value is too low (although the latter case may be less common). A similar effect can been seen for $\gamma_\pm$, where the rescaling increases the value. In Figure 6b there are also cases where the "correction" overshoots (compare filled and open diamonds at the same $\gamma_\pm^{MC} > 0.7$).

Manning's expressions were originally derived for a line charge that was allowed to extend to infinity. If we really want to test the Debye−Hückel approxima-

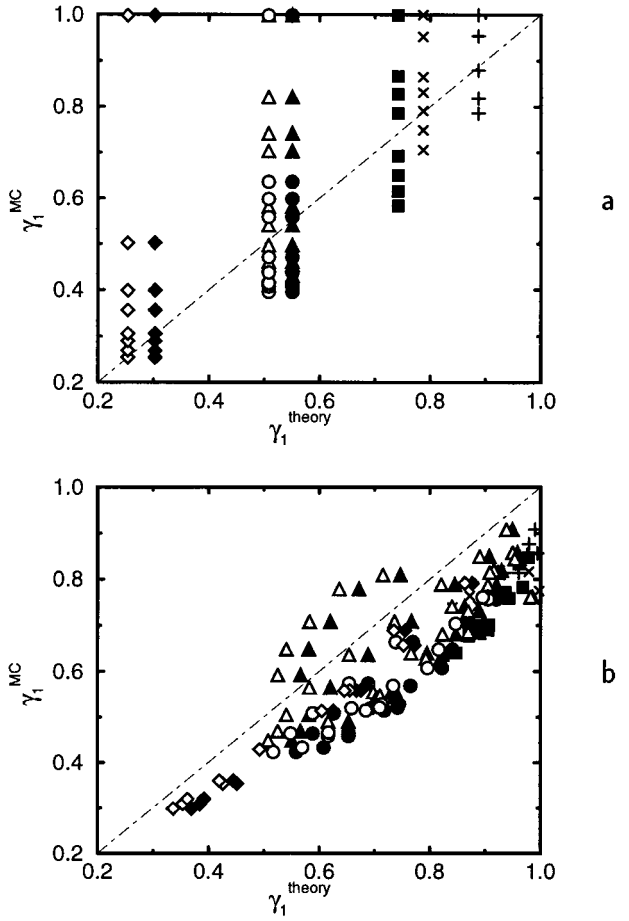

Figure 5. Simulated activity coefficients for the counterions against the value predicted by Manning theory: (a) salt-free system and (b) with added salt. Results are shown for $b = 3$ Å with $\alpha = 0.2$ (× symbols), 0.5 (triangles), and 1.0 (diamonds) and for $b = 6$ Å with $\alpha = 0.2$ (plus signs), 0.5 (squares), and 1.0 (circles). Filled symbols represent the theoretical predictions of eq 10, and open symbols are the corresponding results with Manning rescaling for $\xi > 1$. c_p ranges from 3×10^{-8} to 9.8 mM, and in part b c_s ranges from 7.6×10^{-3} to 100 mM. The dot−dashed line indicates where perfect agreement between theory and simulation would be.

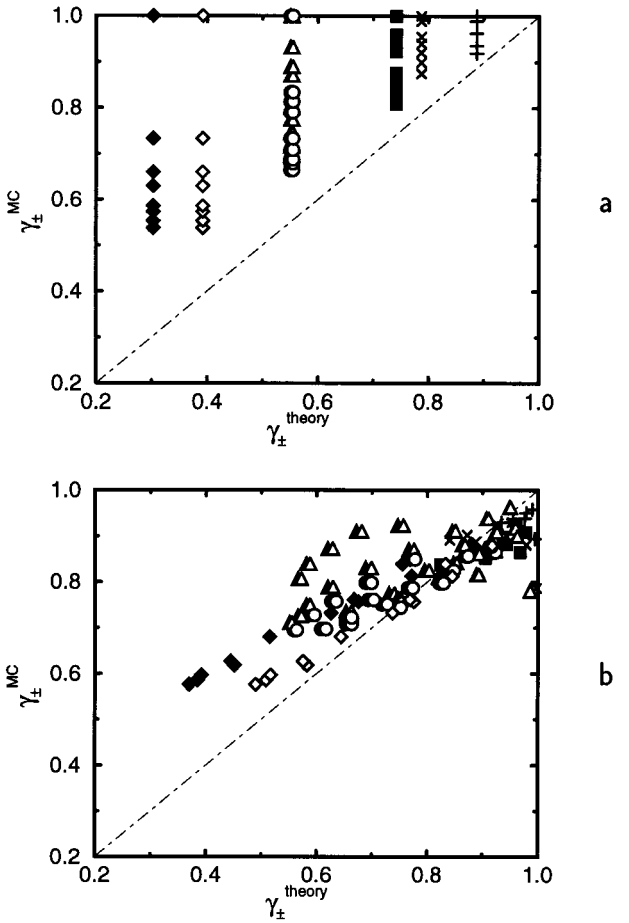

Figure 6. Simulated mean activity coefficients against the value predicted by Manning theory: (a) salt-free system and (b) with added salt. Line and symbols have the same meaning as in Figure 5.

tion, we should perhaps use a more realistic polyelectrolyte model, or at least one that is closer to the simulated model. A step in that direction is to have a finite chain with discrete charges (albeit still a rigid rod) and also include a term for the simple ions:

$$\ln \gamma = -\frac{\kappa l_B}{2} - \frac{2\pi\alpha l_B^2 N_A c_p}{\kappa}\left(\frac{1}{2} + \frac{1}{e^{\kappa b} - 1} + \frac{e^{-N\kappa b} - 1}{N(e^{\kappa b} + e^{-\kappa b} - 2)}\right) \quad (14)$$

with $\kappa^2 = 4\pi l_B N_A 4(c_1 + c_2) = \pi l_B N_A(\alpha c_p + 2c_s)$. We have dropped the subscript since the theory predicts the same value for γ_1, γ_2, and $\gamma_\pm$.

Except for the first term, which is a contribution from just the simple ions without correlations from the macroion, the derivation of this equation (see appendix B) is consistent with that of Manning,[19] which led to eq 10. Manning and Zimm[40] have derived a similar expression (without the N-dependent term), as an expression for $\gamma_\pm$, from Mayer cluster theory by including only the lower order terms, which is equivalent to Debye−Hückel theory.

The first term in eq 14 becomes increasingly significant the higher the ionic strength, the larger the excess of added salt, and the lower the charge density of the chain. It comes from the Debye−Hückel expression for the mean activity coefficient of a simple salt solution.[41−44] Experiments on such solutions (1:1 salt) show that this is a good approximation only up to concentrations of about 10 mM,[45] and the simulations agree. Equation 14 is therefore expected to fail at higher concentrations of added salt. This is illustrated in Figures 8 and 9, where a few points with $c_s = 100$ mM stand out from the rest (marked by arrows). In these cases the first term dominates almost completely.

Including an ion−ion term is in line with the results of Wells[46] and Kakehashi,[47] who found improved agreement with experiment by combining Manning theory with the activity coefficients of the added salt in the absence of the polyelectrolyte and its counterions. Our expression is slightly different, since the counterions from the macroion are included in the ion−ion term through κ.

Manning's infinite line is a special case of the rigid rod used in the derivation of eq 14. If b and α are allowed to go to 0, with the constraints that α/b, αc_p, and $L = Nb$ are constant, and the limit $L \to \infty$ is taken subsequently, the polyelectrolyte part of eq 14 (everything but the first term, the ion−ion term) turns into eq 10. The first step does not change the results significantly as long as the bonds are not overly long. With a maximum bond length of just 6 Å, we could just

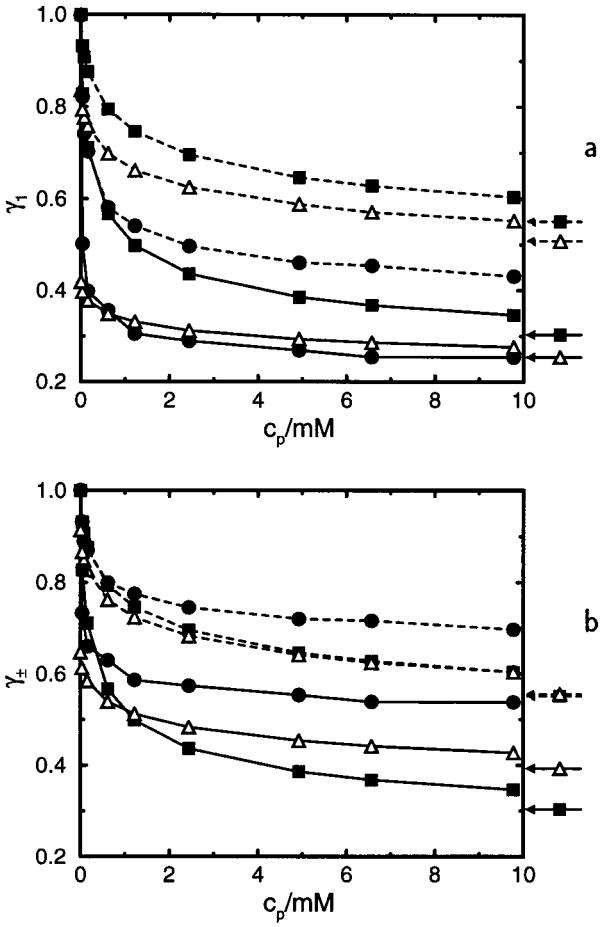

Figure 7. Activity coefficients in the salt-free case as functions of the polyelectrolyte concentration for (a) the counterions and (b) the mean activity coefficient. The bond length is $b = 3$ Å with $\alpha = 0.5$ (dashed lines) and $\alpha = 1$ (solid lines), which gives $\xi = 1.2$ and $\xi = 2.4$, respectively. The symbols inside the frame show the activity coefficients from simulation (circles), the rigid-rod model (eq 14, squares), and the rigid-rod model with Manning rescaling (triangles). The arrows outside mark the constant values predicted by Manning theory, before (eq 12, squares) and after (eq 13, triangles) rescaling.

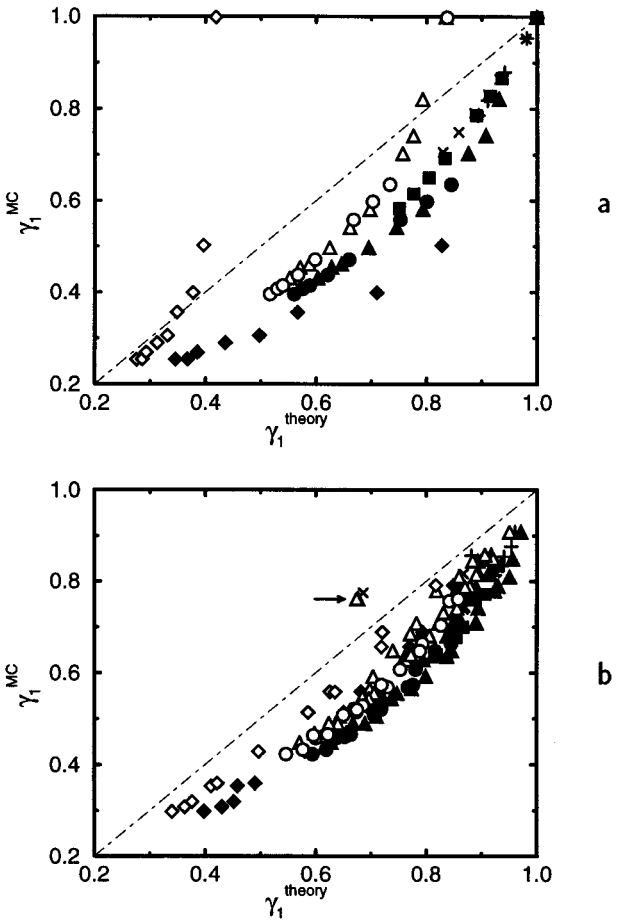

Figure 8. Simulated activity coefficients for the counterions against the value predicted by the discretely charged rigid-rod model: (a) salt-free system and (b) with added salt. The theoretical results are based on eq 14. Otherwise the line and symbols have the same meaning as in Figure 5. The arrow marks three points (× symbol, filled and open triangles) where $c_s = 100$ mM and $c_p = 10$ mM. For all other points, $c_s \leq 10$ mM.

as well have used the continuous line-charge limit, which turns eq 14 into the simplified expression

$$\ln \gamma = -\frac{\kappa l_B}{2} - \frac{2\pi l_B N_A \xi \alpha c_p}{\kappa^3 L}(e^{-\kappa L} + \kappa L - 1) \qquad (15)$$

where αc_p represents the concentration of counterions from the polyelectrolyte.

There is an important difference between a finite and an infinite chain, however. When κ goes to 0, the contribution from the second term in the parentheses of eq 14 corresponds to Manning's result, because $1/(\exp(\kappa b) - 1) \rightarrow 1/(\kappa b)$. In the salt-free case $\kappa^2 = 4\pi l_B N_A \alpha c_p$ and the Manning-like term, including the prefactor, has κ^2 in both numerator and denominator, which cancels to give a constant independent of c_p. In contrast, the *entire* expression within the parentheses, without the prefactor, goes to $N/2$ as $\kappa \rightarrow 0$, and the c_p dependence of the prefactor is retained. The N-dependent term thus ensures that γ goes to 1 when the polyelectrolyte becomes infinitely diluted in the absence of added salt, but for long chains this term is only significant at very low concentrations (small κ).

Tables 1 and 2 also show the results from using eq 14. Graphical representations are given in Figures 7−9. We see that there is no major difference between this equation and the Manning result for γ_1 at moderate additions of salt, but the predictions are more clustered together, and the results for small amounts of added salt no longer stand out. As we have already indicated, there is also a polymer concentration dependence in the salt-free case, although it is still not very good for γ_1. The results for $\gamma_\pm$, on the other hand, are much better, in particular when salt has been added. Equation 14 still has problems at the highest charge densities (when ξ is significantly larger than 1), where the linear response implied by the Debye−Hückel approximation is actually questionable. However, when the system contains added salt and the mean activity coefficient is moderately high, $\gamma_\pm > 0.7$ say, the prediction from eq 14 is quite good.

Although the Manning rescaling generally moves the prediction in the right direction, the conclusion is still that it does not offer a reliable correction. It purports to account for the nonlinear response at high charge densities. This response leads to an accumulation of more counterions around the polyelectrolyte than predicted by the Debye−Hückel approximation, but the fact that the size of the rescaling is not related to the size of

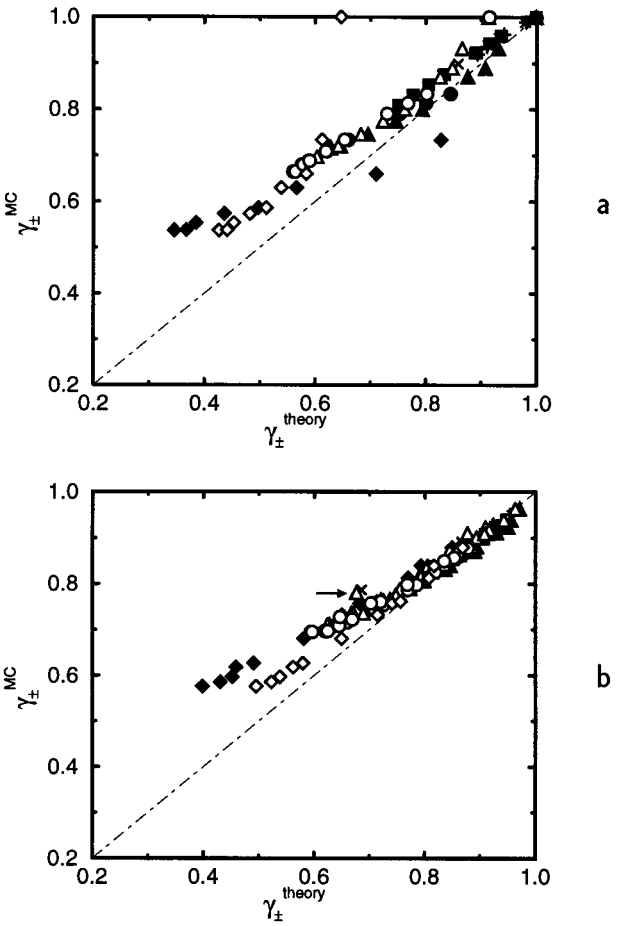

Figure 9. Simulated mean activity coefficients against the value predicted by the discretely charged rigid-rod model: (a) salt-free system and (b) with added salt. The theoretical results are based on eq 14. Otherwise the line and symbols have the same meaning as in Figure 5. The arrow marks three points ($\times$ symbol, filled and open triangles) where $c_s = 100$ mM and $c_p = 10$ mM. For all other points, $c_s \leq 10$ mM.

the error indicates that the nonlinearity is not properly taken care of. This was also the conclusion from comparisons with solutions to the Poisson−Boltzmann equation.[38,39] There are, of course, other effects as well, in particular the fact that the chain is flexible and not a rigid rod, but we interpret the success of eq 14 for $\gamma_\pm$ at the lower charge densities as an indicator that this is not of major concern. In the salt-free case, the Manning rescaling "diverges" at very low polymer concentrations, because the limiting ($c_s = 0$, $c_p \rightarrow 0$) values of γ_1 and $\gamma_\pm$ based on eq 14 are no longer unity, but $\gamma_1' = \xi^{-1}$ and $\gamma_\pm' = \xi^{-1/2}$ (see appendix A).

The fact that the results for $\gamma_\pm$ based on eq 14 are quite reasonable, while those for γ_1 are rather poor, should not come as a complete surprise. We have already mentioned that the Debye−Hückel approximation predicts the same activity coefficients for both counterions and co-ions (as long as no rescaling is performed). In contrast, both our simulations and experiments[48] show a large difference between the activity coefficients of the two species. We should therefore expect the Debye−Hückel result to be a better approximation for the mean activity coefficient $\gamma_\pm$. This was stressed quite strongly by Manning and Zimm, who also estimated a semiquantitative correction for the difference in γ_1 and γ_2,[40]

$$\ln \gamma_1 = \ln \gamma_\pm - \frac{4(\pi\alpha l_B)^3 N_A c_p}{3\sqrt{6}(\kappa b)^2}\mathrm{erfc}(\sqrt{3\kappa\sigma}) \quad (16)$$

where ln $\gamma_\pm$ is obtained from eq 14, σ is a distance of closest approach, and

$$\mathrm{erfc}(x) = \frac{2}{\sqrt{\pi}}\int_x^\infty e^{-t^2}\,dt \quad (17)$$

is the normalized complementary error function. Tables 1 and 2 show that this the correction has a strong tendency to overcompensate and often gives a prediction that is worse than the one it was supposed to correct. Equation 16 is thus not very useful here, not even as a semiquantitative estimate.

To return to our original agenda, i.e., predicting γ_1 for isoionic dilution, we have just argued that this is impossible with the present analytical approach, based on the Debye−Hückel approximation. There are, however, two comments to be made. First, for the low concentrations of polyelectrolyte and added salt investigated here, $\gamma_2 = 1$ is a reasonable approximation, which implies $\gamma_1 = \gamma_\pm^2$. The results for γ_1 using eq 14 as the mean activity coefficient $\gamma_\pm$ are plotted in Figure 10. The agreement is not bad, if we disregard the points where $c_s = 100$ mM and, at least in the salt-free case, the chain with the highest charge density, $\xi = 2.39$ (diamonds). As long as c_p and c_s are at most 10 mM, the simulated value of γ_2 stays in the range 0.90−1.15, while for $c_s = 100$ mM, $\gamma_2 = 0.80$.

Second, the quality of the prediction of γ_1 is not crucial for isoionic dilution, since the experimental curve itself tells if the chosen value was good or bad. If a straight line is obtained when plotting η_r vs c_p, the value was good. If the line is curved, it was not, but the results can still indicate how to proceed by trial and error. All we need is an initial guess. As such the Manning prediction has been remarkably successful for vinylic polyelectrolytes.[4,9,10]

Looking at the salt-free simulations, Figures 5a and 6a, we see that Manning theory is actually better for γ_1 than for $\gamma_\pm$ in one respect. It is able to at least get γ_1 right occasionally (fortuitously), while $\gamma_\pm$ is consistently underestimated. For example, for $b = 3$ Å Manning theory happens to be in reasonable agreement toward the higher polyelectrolyte concentrations in the salt-free case. This bond length is close to the value normally used for poly(acrylic acid), i.e., 2.52 Å, and our initial macroion concentrations were in fact inspired by experiments on this polyelectrolyte, where Manning theory was able to predict the effective ionic strength (cf. Figure 12).[4,10] The apparent experimental success can thus be explained, and the Manning expressions may be used for γ_1 as empirical rules, at least for vinylic polyelectrolytes. It should be borne in mind, however, that it is not theoretically justified to use the Manning results as a general theory for γ_1. Its applicability as an empirical rule has to be tested separately for different polyelectrolytes and concentrations.

Viscosity Theory: Intramolecular Interactions. The conformational interpretation of the polyelectrolyte effect has led to the hypothesis that the average conformation is kept constant during an isoionic dilution, which we have shown to be correct. The fact that the intramolecular interactions are constant does not

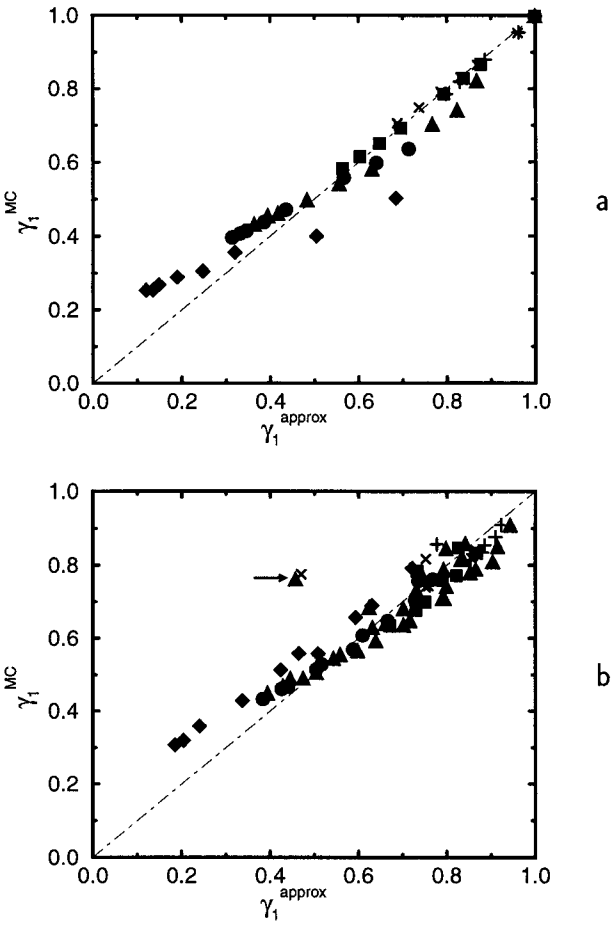

Figure 10. Simulated activity coefficients for the counterions against an approximation assuming $\gamma_2 = 1$: (a) salt-free system and (b) with added salt. With this approximation, $\gamma_1^{approx} = \gamma_\pm^2$, where the mean activity coefficient is taken from eq 14. Otherwise the line and symbols have the same meaning as in Figure 5. The arrow marks two points (× symbol and triangle) where $c_s = 100$ mM and $c_p = 10$ mM. For all other points, $c_s \leq 10$ mM.

prove that they are responsible for the polyelectrolyte effect, however. The isoionic dilution may also keep the intermolecular interactions constant. We will now use a theoretical expression for the reduced viscosity, based solely on a conformational interpretation, to see if the simulated conformational changes can reproduce the qualitative features of experimental viscosity curves. It should be made perfectly clear that we have not simulated the viscosity; we are only using our simulation results as input to a theory that expresses the viscosity in terms of properties that can be obtained from a single-chain simulation. To be specific, the simulations supply the radius of gyration as a function of the polyelectrolyte concentration for different dilution series, where the diluent has a given ionic strength.

Reed has shown that it is possible to obtain a peak in η_r vs c_p by combining the classical concept of a viscometrically equivalent sphere, the radius of gyration of a wormlike chain and an empirical expression for the total persistence length.[49] We will stop at the first step with the hydrodynamic radius proportional to the simulated radius of gyration, i.e., $R_H = \zeta R_G$. Taking the Einstein relation for a suspension of spheres, $\eta_r c_p = 2.5\phi$,[50] and calculating the volume fraction as $\phi = 4\pi(\zeta R_G)^3 N_A c_p/(3N)$, we get the intrinsic viscosity

$$[\eta] = \frac{10\pi(\zeta R_G)^3 N_A}{3N} \tag{18}$$

and the Huggins equation becomes

$$\eta_r = \frac{10\pi(\zeta R_G)^3 N_A}{3N} + k_H\left(\frac{10\pi(\zeta R_G)^3 N_A}{3N}\right)^2 c_p \tag{19}$$

This represents a prediction of the reduced viscosity based purely on the chain dimensions.

For the proportionality constant between the hydrodynamic radius and the radius of gyration, Reed used $\zeta = 0.85$ and the Huggins coefficient k_H was set equal to 1. With these values, simulations give the results shown in Figure 11, which should be compared to typical experimental curves. An example of such a curve is given in Figure 12, and a similar behavior can be seen in Figure 2 of ref 3. The system in Figure 11 roughly corresponds to that in Figure 12. The other model

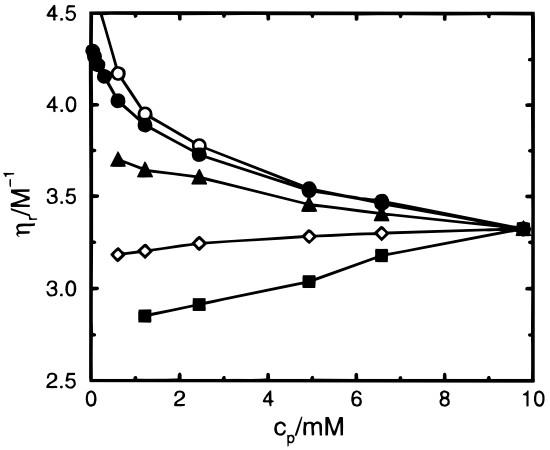

Figure 11. Change in reduced viscosity predicted by eq 19 for $b = 3$ Å and $\alpha = 0.5$. Diamonds represent isoionic dilution with a 2.1 mM salt solution. The salt concentrations of the other diluents are 0 mM (open circles), 0.1 mM (filled circles), 0.5 mM (filled triangles), and 5 mM (filled squares).

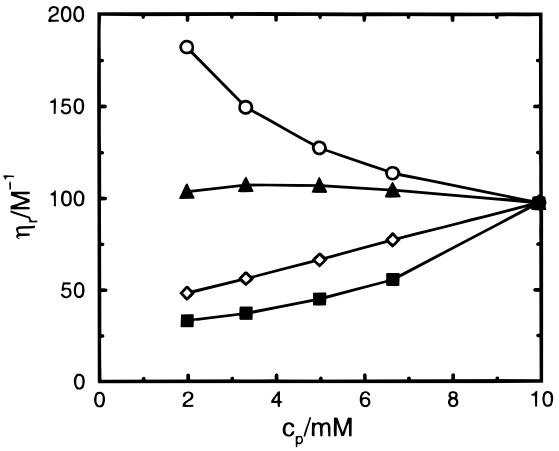

Figure 12. Experimental results for the reduced viscosity of poly(acrylic acid) with $\alpha = 0.5$ and a molecular weight of 42 000 in the acid form (misprint in the original article), which corresponds to $N = 583$. The monomer distance along the backbone is 2.52 Å. The figure is reproduced from the data in Figure 5 of ref 4 with the units converted from mass concentrations to molar concentrations. The symbols are the same as in Figure 11, including the isoionic concentration of 2.1 mM.

systems give qualitatively very similar results, including the one with $b = 6$ Å and $\alpha = 1$, which displays largest relative expansion according to Figure 3.

In Figure 11, there is an increase in the reduced viscosity when the chain expands, but it is qualitatively different from the experimental results. Except for the lowest ionic strengths, the slopes of the curves hardly change with dilution, as they do in Figure 12 (not counting the isoionic dilution), and there is not a hint of a maximum. We can get a more pronounced curvature if we add κ^{-1} to the radius of gyration to include the electrical double layer in an effective hydrodynamic radius, as was suggested,[49] but that would mean that we are no longer looking at just the conformational expansion but also including some other form of interaction.

However, it is not entirely fair to pass judgment on eq 19 based on our simulation data, since an 80-mer is rather short and the Debye length, κ^{-1}, is of the order of the chain dimensions at the initial point. For $b = 3$ Å and $\alpha = 0.5$, $\kappa R_G = 0.7$ initially, and for $b = 6$ Å and $\alpha = 1.0$, the corresponding value is 1.3. This means that the radius of gyration varies only slowly with the ionic strength, which is readily seen in Figures 3 and 4. All we can say is that intermolecular interactions should dominate for short chains.

For longer chains we would expect a larger conformational contribution, which is to what the investigation of Reed corresponds.[49] He expressed the persistence length as

$$l_p = A + B/\sqrt{I} \tag{20}$$

where A and B are empirical constants and I is an effective ionic strength. Theoretically, A corresponds to the intrinsic persistence length, and the second term is the electrostatic persistence length. It is easily seen from simulations that the $1/\sqrt{I}$ dependence is only valid when κR_G is significantly larger than 1,[51] which, as already discussed, is not the case here. Our results are therefore not really comparable to those of Reed.

Viscosity Theory: Intermolecular Interactions. Since the conformational theory did not give a qualitatively correct behavior, we stated that the viscosity of short chains, like ours, should be governed mainly by intermolecular interactions, but this remains to be tested. There are no macroion−macroion interactions in the simulations, but these have been taken into account in an expression derived by Hess and Klein for charged Brownian spheres,[52]

$$\eta_r = \frac{R_H(\pi\alpha^2 l_B N_A)^2 c_p}{10\kappa^3} \tag{21}$$

This equation has a number of features that make it look promising. For example, if the hydrodynamic radius, R_H, and κ are kept fixed, η_r depends linearly on c_p (α and l_B are constant), i.e., isoionic dilution is provided for. Since κ, as defined in eq 14, may change during an isoionic dilution where the average chain size is constant, we will instead use an effective value. For a solution of a simple salt, the Debye−Hückel parameter can be expressed as $\kappa = \sqrt{8\pi l_B N_A I}$. We will simply replace the ionic strength in this definition with $I_{eff} = \gamma_1 c_1$, which we have shown to be conserved during isoionic dilution, and use the effective interaction parameter $\kappa_{eff} = \sqrt{8\pi l_B N_A \gamma_1 c_1}$.

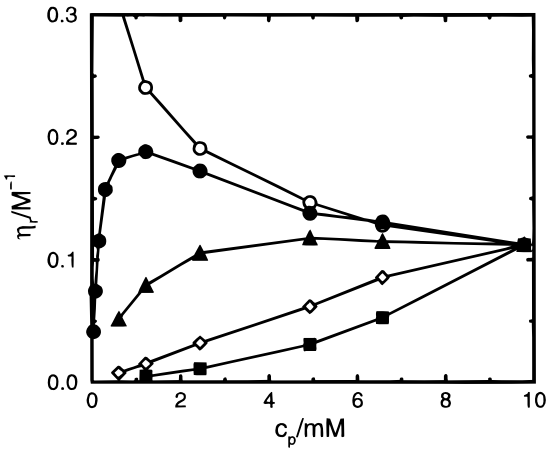

Figure 13. Change in reduced viscosity predicted by eq 21 for the same cases as in Figure 11.

Furthermore, in a series of viscosity measurements using isoionic dilution, Bokias and Staikos found the second term in the Huggins equation (eq 1) to be proportional to $I_{eff}^{-1.3}$,[4] which would correspond to $\kappa_{eff}^{-2.6}$. κ^{-3} in eq 21 therefore appears to be qualitatively correct. On the other hand, other charge dependencies have been suggested, both theoretically[12] and experimentally,[4] but since we will only look at the qualitative features of dilution curves where the degree of dissociation is constant, the exact dependence on α is not important as long as it can be factored out.

Figure 13 shows the result of using eq 21 to calculate η_r from our simulation data, where we have used κ_{eff} and $R_H = 0.85\ R_G$, as in the evaluation of the conformationally based expression, eq 19. With all the qualitatively correct features in place in eq 21, it is not really surprising that our hypothetical viscosity curves look like experimental ones, represented here by Figure 12.

Quantitatively there is still something left to be desired. The model parameters and concentrations in Figure 13 are similar to those of the real system in Figure 12, but η_r differs by roughly 3 orders of magnitude. About 1 order of magnitude can be accounted for by the fact that the number of monomers is 7 times larger in the experimental polyelectrolyte, but the rest should come from the theory. We have already mentioned that there have been theoretical arguments for a different α dependence (α^2 instead of α^4), and this would also include an unknown numerical constant.[12]

Equation 21 does not have an intrinsic viscosity, but we could add the effective hard-sphere result given in eq 18. Actually, it would make sense to add the whole conformationally based expression eq 19 to the right-hand side of eq 21, but we would need to find a constant to balance the intramolecular and intermolecular contributions. As can be seen from Figures 11 and 13, the two equations differ by about 1 order of magnitude. Antonietti et al. have used such a combination of expressions to fit experimental data.[17]

There is an interesting observation to be made in this context. It has been found, both experimentally and theoretically, that the electrostatic persistence length is proportional to the (effective) Debye length, κ^{-1}, for flexible chains (cf. eq 20, $\kappa \propto \sqrt{I}$), at least if the persistence length is defined so that it is proportional

to the square of the end-to-end distance or (under certain conditions) the square of the radius of gyration.[51] When the intrinsic persistence length is negligible, this implies $R_G \propto 1/\sqrt{\kappa}$, which would make the second term in eq 19 proportional to κ^{-3}, just as in eq 21.

Conclusions

We set out to see if an isoionic dilution could keep the average chain conformation constant and to what extent a Debye−Hückel description could be used to predict the required ionic strength.

The results show that, with an effective ionic strength based on the activity of the counterions, it is indeed possible to retain the average conformation on dilution. This does not prove that chain expansion is the main determinant of the polyelectrolyte effect, only that interactions are kept constant.

In fact, we have used the simulation results as input for a theoretical expression based on the average chain dimensions, and we were not able to reproduce the qualitative features of the experimentally observed behavior of the reduced viscosity as a function of the polyelectrolyte concentration. Another theoretical expression for η_r, which takes intermolecular interactions into account, does give qualitatively correct behavior. It should be pointed out, though, that our 80-mers are really too short to honestly probe any major conformational contribution to η_r, because κR_G is never much larger than 1, which means that there is not much room for any larger variations in the intramolecular interactions, and as a consequence, the chain neither expands nor contracts to any great extent. The conclusion is that the polyelectrolyte effect should be dominated by intermolecular interactions for short chains ($\kappa R_G \leq 1$), but our results do not say anything about long chains.

There is a fundamental problem involved in predicting the counterion activity from the Debye−Hückel approximation, since, at best, it should give the mean activity coefficient rather than γ_1. For the purpose of calculating $\gamma_\pm$, the infinite line charge model used by Manning often gives poor agreement with simulation. Much better in this respect is to use a rigid rod of finite length and including a separate contribution from the simple ions, eq 14, provided that the charge density and the concentrations of polyelectrolyte and added salt are not too high. Rough upper limits for the applicability of eq 14 are $\xi = 1$, $c_p = 10$ mM, and $c_s = 10$ mM. Some added salt is better than an absolutely salt-free system. With the assumption that $\gamma_2 = 1$, the mean activity coefficient from the rigid-rod model, eq 14, gives a reasonable approximation for the activity coefficients of the counterions in the form $\gamma_1 = \gamma_\pm^2$, with limitations similar to those just stated.

The "correction" offered by a Manning rescaling when $\xi > 1$, is correlated with neither the size nor the sign of the error in the activity coefficient and is therefore of limited use. The original Manning theory has proved useful experimentally when predicting γ_1 for isoionic dilution.[4,9,10] This is shown to be fortuitous, but it means that Manning theory can be used as an empirical rule for this purpose, at least for vinylic polyelectrolytes.

Acknowledgment. M.U. would like to thank Jonathan Ennis-King, Bo Jönsson, and Cliff Woodward for long and valuable discussions and Malek Khan for code swapping. This work was supported by the European Union, Contract No. ERBCHRX-CT94-0655.

Appendix A

In this appendix we show how the activity coefficients in a polyelectrolyte solution are calculated using Manning rescaling. This summarizes the procedure originally described by Manning in ref 19.

Two basic assumptions of Manning theory are that the Debye−Hückel approximation remains valid for charge densities $\xi \leq 1$ and that the same expressions can be used for $\xi > 1$, if a constant, effective value of $\xi' = 1$ is used. The rescaling can equivalently be expressed as setting the degree of dissociation to $\alpha' = b/l_B$.

Starting with the counterions, in the rescaled system their activity is $a_1' = \gamma_1(\alpha')c_1' = \gamma_1(\alpha')(\alpha' c_p + c_s)$, where $\gamma_1(\alpha')$ is the result of using α' in the Debye−Hückel expression, for example, eq 10 or 14 (with $\kappa^2 = 4\pi l_B N_A(\alpha' c_p + 2c_s)$). The assumption is that the *activity* in the actual system is the same as in the rescaled system, but since the actual counterion concentration is $\alpha c_p + c_s$, we get the new, rescaled *activity coefficient*

$$\gamma_1' = \frac{a_1'}{c_1} = \gamma_1(\alpha')\frac{\alpha' c_p + c_s}{\alpha c_p + c_s} \tag{22}$$

Similarly, for the co-ions in the actual system, we have

$$\gamma_2' = \gamma_2(\alpha')\frac{c_s}{c_s} = \gamma_1(\alpha') \tag{23}$$

where the last equality uses the fact that the Debye−Hückel approximation leads to the same activity coefficient for both counterions and co-ions.

Finally, it should be noted that while eq 14 gives $\gamma = 1$ for $c_s = 0$ and $c_p \to 0$, and thus $\gamma_1(\alpha') = 1$, Manning rescaling leads to

$$\gamma_1' = \alpha'_1/\alpha = \xi^{-1} \tag{24}$$

and

$$\gamma_\pm' = \sqrt{\gamma_1'\gamma_2'} = \xi^{-1/2} \tag{25}$$

Appendix B

In this appendix we derive an expression for the activity coefficients of the simple ions in a solution around a rigid rod with N discrete charges, which have a valency z_p and are separated by bonds of length b. We will also include a term from the (monovalent) simple ions themselves.

We start by making the assumption that the total excess (electrostatic) free energy per unit volume, $\tilde{F}^{el} \equiv \beta F^{el}/V$, can be separated into a contribution from the simple ions, without the correlations arising from the macroion, and a contribution from the excess chemical potential of the polyelectrolyte divided by the volume,

$$\tilde{F}^{el} = \tilde{F}_{12}^{\tilde{e}l} + \beta\mu_p^{el}/V \tag{26}$$

Next we assume that both contributions can be calculated within the Debye−Hückel approximation using point charges.[41−44]

With the charge of the macroion spread out to form a constant, neutralizing background, the first term is

$$\tilde{F}_{12}^{el} = -\frac{\kappa^3}{12\pi} \tag{27}$$

where κ is defined as $\kappa^2 = 4\pi l_B N_A(c_1 + c_2) = 4\pi l_B N_A(|z_p|c_p + 2c_s)$.

For the electrostatic part of the chemical potential of the polyelectrolyte, we use the Güntelberg charging process, where the charges on the monomers are simultaneously increased from 0 to $z_p e$, with the help of a charging parameter λ going from 0 to 1. During the process each monomer i feels the average potential, $\bar{\psi}_i(\lambda)$, from the rest of the system. The

simple ions are fully charged, but their positions are preaveraged and in the Debye−Hückel approximation they only enter through κ. At i the contribution from monomer j is

$$\psi(r_{ij},\lambda) = \frac{z_p e\lambda}{4\pi\epsilon_r\epsilon_0}\left(\frac{e^{-\kappa r_{ij}}}{r_{ij}} - \frac{1}{r_{ij}}\right) \tag{28}$$

where we have subtracted the direct interaction of the monomers from the screened Coulomb potential since we have chosen to view the rigid rod as a single particle rather than treating the monomers separately. This is not very important since the interaction of the rigid rod with itself is independent of the simple ions and will not affect their activity coefficients in the end.

The electrostatic work, dw_i, to give monomer i a small amount of charge $d(z_p e\lambda)$ is $\bar{\psi}_i(\lambda) z_p e\, d\lambda$, and the total work of charging the polyelectrolyte, i.e., the electrostatic contribution to its chemical potential, is

$$\beta\mu_p^{el} = z_p e\int_0^1 \lambda\, d\lambda \sum_{i=1}^{N}\bar{\psi}_i(\lambda) = \int_0^1 d\lambda \sum_{i=1}^{N}\sum_{j=1}^{N} {z_p}^2 l_B\left(\frac{e^{-\kappa r_{ij}}}{r_{ij}} - \frac{1}{r_{ij}}\right)$$

$$= -\frac{N z_p^2 \kappa l_B}{2} + \sum_{k=1}^{N-1}(N-k)\frac{z_p^2 l_B}{kb}(e^{-\kappa k b} - 1) \tag{29}$$

where we have singled out the N terms for the monomers interacting with their own ion atmospheres and then collected the remaining terms as the $2(N - k)$ contributions from interactions between monomers separated by k bonds.

To obtain the activity coefficients of the simple ions from the electrostatic free energy per unit volume, we need only to take the derivative with respect to the number density of ion species l (1 or 2), $N_A c_l$. Noting that the volume per polyelectrolyte can be written $N/(N_A c_p)$ and that

$$\frac{\partial\kappa}{N_A \partial c_l} = \frac{2\pi l_B}{\kappa} \tag{30}$$

we get

$$\ln\gamma_l = \beta\mu_l^{el} = \frac{\partial\tilde{F}^{el}}{N_A\partial c_l} = \frac{\partial\tilde{F}_{12}^{el}}{\partial\kappa}\frac{\partial\kappa}{N_A\partial c_l} + \frac{\partial}{\partial\kappa}\left(\frac{c_p\beta\mu_p^{el}}{N}\right)\frac{\partial\kappa}{\partial c_l} =$$

$$= -\frac{\kappa l_B}{2} - \frac{\pi z_p^2 l_B^2 N_A c_p}{\kappa} - \frac{2\pi z_p^2 l_B^2 N_A c_p}{N\kappa}\sum_{k=1}^{N-1}(N-k)e^{-\kappa k b} =$$

$$= -\frac{\kappa l_B}{2} - \frac{2\pi z_p^2 l_B^2 N_A c_p}{\kappa}\left(\frac{1}{2} + \frac{1}{e^{\kappa b} - 1} + \frac{e^{-N\kappa b} - 1}{N(e^{\kappa b} + e^{-\kappa b} - 2)}\right) \tag{31}$$

References and Notes

(1) Huggins, M. L. *J. Am. Chem. Soc.* **1942**, *64*, 2716.
(2) Eisenberg, H.; Pouyet, J. *J. Polym. Sci.* **1954**, *13*, 85.
(3) Terayama, H.; Wall, F. T. *J. Polym. Sci.* **1955**, *16*, 357.
(4) Bokias, G.; Staikos, G. *Polymer* **1995**, *36*, 2079.
(5) Pals, D. T. F.; Hermans, J. J. *J. Polym. Sci.* **1950**, *5*, 733.
(6) Pals, D. T. F.; Hermans, J. J. *Recl. Trav. Chim. Pays-Bas* **1952**, *71*, 433.
(7) Flory, P. J. *Principles of Polymer Chemistry*; Cornell University Press: Ithaca, 1992.
(8) Yamakawa, H. *Modern Theory of Polymer Solutions*; Harper and Row: New York, 1971.
(9) Davis, R. M.; Russel, W. B. *Macromolecules* **1987**, *20*, 518.
(10) Staikos, G.; Bokias, G. *Polym. Int.* **1993**, *31*, 385.
(11) Rosen, B.; Kamath, P.; Eirich, F. *Discuss. Faraday Soc.* **1952**, *11*, 135.
(12) Cohen, J.; Priel, Z.; Rabin, Y. *J. Chem. Phys.* **1988**, *88*, 7111.
(13) Cohen, J.; Priel, Z. *Polym. Commun.* **1989**, *30*, 223.
(14) Yamanaka, J.; Matsuoka, H.; Kitano, H.; Ise, N.; Yamaguchi, T.; Saeki, S.; Tsubokawa, M. *Langmuir* **1991**, *7*, 1928.
(15) Yamanaka, J.; Yamada, S.; Ise, N.; Yamaguchi, T. *J. Polym. Sci., Polym. Phys. Ed.* **1995**, *33*, 1523.
(16) Wu, J.; Wang, Y.; Hara, M.; Granville, M.; Jerome, R. J. *Macromolecules* **1994**, *27*, 1195.
(17) Antonietti, M.; Briel, A.; Förster, S. *J. Chem. Phys.* **1996**, *105*, 7795.
(18) Russel, W. B. *J. Chem. Soc. Faraday Trans. 2* **1984**, *80*, 31.
(19) Manning, G. S. *J. Chem. Phys.* **1969**, *51*, 924.
(20) Alfrey, T., Jr.; Berg, P. W.; Morawetz, H. *J. Polym. Sci.* **1951**, *7*, 543.
(21) Fuoss, R. M.; Katchalsky, A.; Lifson, S. *Proc. Natl. Acad. Sci. U.S.A.* **1951**, *37*, 579.
(22) Marcus, R. A. *J. Chem. Phys.* **1955**, *23*, 1057.
(23) Wennerström, H.; Jönsson, B.; Linse, P. *J. Chem. Phys.* **1982**, *76*, 4665.
(24) Reed, C. E.; Reed, W. F. *J. Chem. Phys.* **1991**, *94*, 8479.
(25) Ullner, M.; Jönsson, B. *Macromolecules* **1996**, *29*, 6645.
(26) Linse, P.; Jönsson, B. *J. Chem. Phys.* **1983**, *78*, 3167.
(27) Metropolis, N. A.; Rosenbluth, A. W.; Rosenbluth, M. N.; Teller, A.; Teller, E. *J. Chem. Phys.* **1953**, *21*, 1087.
(28) Lal, M. *Mol. Phys.* **1969**, *17*, 57.
(29) Madras, N.; Sokal, A. D. *J. Stat. Phys.* **1988**, *50*, 109.
(30) Ullner, M.; Jönsson, B.; Söderberg, B.; Peterson, C. *J. Chem. Phys.* **1996**, *104*, 3048.
(31) Christos, G. A.; Carnie, S. L. *J. Chem. Phys.* **1990**, *92*, 7661.
(32) Gordon, H. L.; Valleau, J. P. *Mol. Sim.* **1995**, *14*, 361.
(33) Widom, B. *J. Chem. Phys.* **1963**, *39*, 2808.
(34) Svensson, B.; Woodward, C. E. *Mol. Phys.* **1988**, *64*, 247.
(35) Press, W. P.; Flannery, B. P.; Teukolsky, S. A.; Vettering, W. T. *Numerical Recipes, The Art of Scientific Computing*; Cambridge University Press: Cambridge, 1986.
(36) Linse, P.; Gunnarsson, G.; Jönsson, B. *J. Phys. Chem.* **1982**, *86*, 413.
(37) Manning, G. S. *Acc. Chem. Res.* **1979**, *12*, 443.
(38) Fixman, M. *J. Chem. Phys.* **1979**, *70*, 4995.
(39) Le Bret, M.; Zimm, B. H. *Biopolymers* **1984**, *23*, 287.
(40) Manning, G. S.; Zimm, B. H. *J. Chem. Phys.* **1965**, *43*, 4250.
(41) Debye, P.; Hückel, E. *Phys. Z.* **1923**, *24*, 185.
(42) Fowler, R. H.; Guggenheim, E. A. *Statistical Thermodynamics*; Cambridge University Press: Norwich, 1960.
(43) Davidson, N. *Statistical Mechanics*; McGraw-Hill: New York, 1962.
(44) McQuarrie, D. A. *Statistical Mechanics*; Harper Collins: New York, 1976.
(45) Scatchard, G.; Prentiss, S. S. *J. Am. Chem. Soc.* **1933**, *55*, 4355.
(46) Wells, J. D. *Biopolymers* **1973**, *12*, 223.
(47) Kakehashi, R. *Bull. Chem. Soc. Jpn.* **1996**, *69*, 3075.
(48) Nagasawa, M.; Izumi, M.; Kagawa, I. *J. Polym. Sci.* **1959**, *37*, 375.
(49) Reed, W. F. *J. Chem. Phys.* **1994**, *101*, 2515.
(50) Einstein, A. *Ann. Phys.* **1906**, *19*, *289*.
(51) Ullner, M.; Jönsson, B.; Peterson, C.; Sommelius, O.; Söderberg, B. *J. Chem. Phys.* **1997**, *107*, 1279.
(52) Hess, W.; Klein, R. *Adv. Phys.* **1983**, *32*, 173.

MA9804388